A Real-time Arrhythmia Heartbeats Classification Algorithm using Parallel Delta Modulations and Rotated Linear-Kernel Support Vector Machines

Xiaochen Tang, *Student Member, IEEE*, Ziwei Ma, Qisong Hu, *Student Member, IEEE*, Wei Tang, *Member, IEEE*

***Abstract*—Real-time wearable electrocardiogram(ECG) monitoring sensor is one of the best candidates in assisting cardiovascular disease(CVD) diagnosis. In this paper, we present a novel real-time machine learning system for Arrhythmia classification. The system is based on the parallel Delta modulation and QRS/PT wave detection algorithms. We propose a patient dependent rotated linear-kernel support vector machine (SVM) classifier that combines the global and local classifiers, with three types of feature vectors extracted directly from the Delta modulated bit-streams. The performance of the proposed system is evaluated using the MIT-BIH Arrhythmia Database. According to the AAMI standard, two binary classifications are performed and evaluated, which are supraventricular ectopic beat(SVEB) versus the rest four classes, and ventricular ectopic beat(VEB) versus the rest. For SVEB classification, the preferred SkP-32 method's F1 score, sensitivity, specificity and positive predictivity value are 0.83, 79.3%, 99.6% and 88.2%, respectively, and for VEB classification, the numbers are 0.92, 92.8%, 99.4% and 91.6%, respectively. The results show that the performance of our proposed approach is comparable to that of published research. The proposed low-complexity algorithm has the potential to be implemented as an on-sensor machine learning solution.**

***Index Terms*—ECG, parallel delta modulator, SVM.**

I. Introduction

According to the World Health Organization(WHO)'s statistics, people die each year from CVDs, holds estimated 31% of all deaths worldwide, and it has been recognized as the leading health problem in many countries [1]. American Heart Association's report shows that $329.7 billion was spent on CVD and stroke in the United States annually directly and indirectly, which includes $199.2 direct expenditures [2]. Though CVDs seem as the leading-cause-of-death diseases, study shows that estimated 90% heart attacks are preventable [3], if people could control the risk factors beginning in youth: preventing obesity, smoking cessation, etc. Timely diagnosis is also crucial, and ECG is one of the necessary methods for diagnosing CVDs. Among the CVDs, Arrhythmia is an important portion, and if there is no timely treatment, acute arrhythmic symptoms may cause high death rate. Even for some arrhythmias that are not looming life-threatening, patients may need medical care or attention for preventing future health deterioration. Therefore continuous ECG monitoring is needed by patients and even by normal people with uncomfortable heart feelings. Most doctor's choice for continuous ECG monitoring is the Holter monitor, it usually records patient's ECG data for 24 to 48 hours, but the Holter monitor system cannot perform diagnosis in real time and only the data of recorded period is analyzed, if there were severe Arrhythmic heart beats happening during recording or Arrhythmic heart beats happen outside the recorded episode, patients cannot get timely warning or medical care, so continuous ECG monitoring in real time is needed and wearable ECG sensors in wireless body sensor network(WBSN) become one of the best candidates.

Lots of research efforts have been done in designing wearable ECG sensors [4]–[7], most of the researches have ability to detect QRS complexes and transmit ECG data to a remote center for real time ECG monitoring. However, in this era of big data, more data has been created in the past two years than the entire human history [8], and the scenario of the significantly increased computation and data transmission requirement makes the wearable ECG sensors with the ability of processing data locally an eager option. Researches designed for detecting Arrhythmias usually process data in two main steps, QRS complex detection and the following Arrhythmia classification based on extracted features from the detected heart beat data [9]–[13], and power consumption should be taken into account in designing the classifiers, since wearable ECG sensors cannot afford power hungry circuits, for example, researches [10], [14], [15], are high performance classifiers but are not suitable to be implemented inside the wearable sensors.

Machine learning has recently been applied to continuous monitoring of physiological signals for on-sensor processing [16]. Due to latency, security, and privacy requirement, on-sensor processing rather than sending the raw data to the cloud is preferred in medical devices [8]. Most of the wearable sensors need to keep the power consumption in the level of milliwatts (mW) or less in order to keep a reasonable the battery lifetime [17], [18]. However, to implement deep learning inference using neural network would consume hundreds of mW due to the intensive multiply-and-accumulate (MAC) operations and the data movement between memory and the processing unit [8]. Therefore, a machine learning algorithm that can accommodate real-time processing without too much data storage and movement is preferred in wearable sensor applications.

In this paper, we present a real-time machine learning system based on parallel delta modulation to perform classification of normal heartbeats and Arrhythmic heartbeats with

This work is sponsored by United States National Science Foundation grant 1652944.

Xiaochen Tang, Qisong Hu, and Wei Tang are with the Klipsch School of Electrical and Computer Engineering, New Mexico State University, USA.

Ziwei Ma is with the Department of Mathematical Sciences, New Mexico State University, USA.

Correspondence should be addressed to: Wei Tang 1125 Frenger Mall, Las Cruces, New Mexico 88003 USA. E-mail: wtang@nmsu.edu

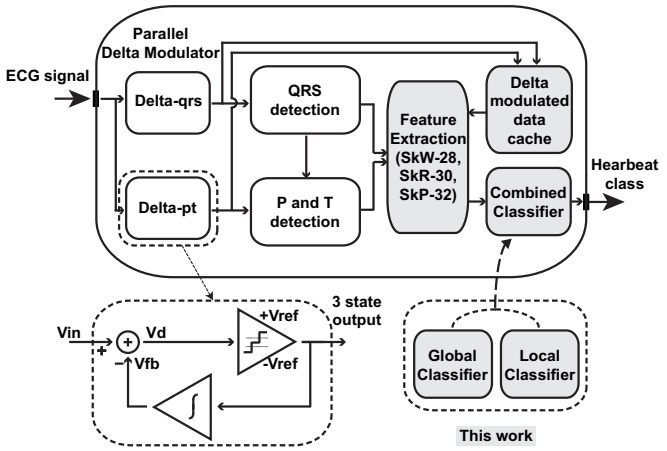

Fig. 1. The proposed real-time Arrhythmia classification system. After parallel Delta modulation and QRS/PT wave detection, this work emphasizes new Feature Extraction and Combined Classifier design.

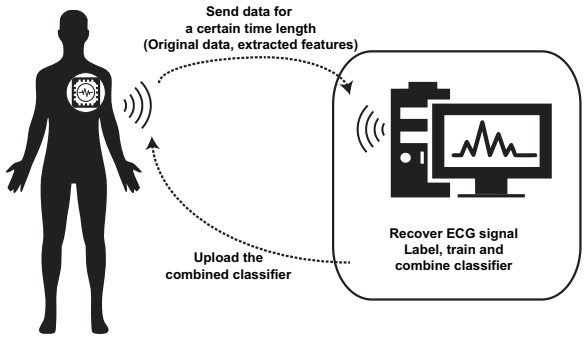

Fig. 2. The proposed system applied in future practice scenario, training on computers, low power consuming Arrhythmia heartbeats classification on wearable sensor.

AAMI standard [19]. The system is based on our previous work of parallel delta modulation based QRS and PT detection system [20]. As illustrated in Fig. 1, the proposed system first converts the input ECG signals into Delta modulated bit-streams using parallel Delta modulators, then the QRS complex, P wave, and T wave are detected from the bit-streams using Local Maximum or Minimum Point algorithms. In this paper, following the detected wave information, features can be directly extracted from the bit-streams using the proposed Feature Extraction algorithm (SkW, SkR, SkP), then the Combined Classifier performs classification of the Arrhythmic heartbeats.

In the future application scenario, the proposed system are designed to perform training on computers that contains most of the computation, then upload the combined classifier back to the wearable sensor for continuously monitoring and classifications as shown in Fig. 2. Cooperating with communication circuits [21]–[23], collected delta modulated ECG data for a certain time length, with information from QRS/PT detection algorithm and extracted features are sent out to a base station. Meantime at the base station, ECG signals are recovered and labeled by certified technicians and powerful automatic algorithms that do not need to care power consumptions, then the local classifier could be trained with the labeled data. With the proposed method, the combined classifier is computed and sent back to the sensor, thus the sensor could keep performing classifications at a very low power consuming level, and only classified Arrhythmia beats are recorded and sent out for a secondary certification if needed, which could reduce huge transmission power compared to transmitting all the data.

The main contributions of this paper are (1) proposed a new ECG machine learning algorithm including feature extraction and inference based on Parallel Delta modulation, (2) proposed a patient dependent rotation SVM classifier to identify Arrhythmias, which utilizes the linear kernel to reduce hardware cost, and (3) evaluated the performance of the proposed method in SVEB and VEB classification using the MIT-IBH database and compared with other reported algorithms. Due to the low complexity operation, the overall system has the potential to be implemented on the sensor circuits. The paper is organized as follows: Section II describes the ECG database and the challenges in ECG classification. Section III presents the structure of the parallel Delta modulation based sampler and the QRS/PT detection algorithm. Section IV provides the proposed rotation support vector machine classifier and the proposed extracted feature vectors. The performance evaluation results and the corresponding comparison with other published literatures are shown in Section V. Finally, Section VI concludes the paper.

II. Heartbeat classification challenge and ECG data description

ECG signal classification is a difficult challenge because of the large interpatient and intrapatient morphology variation of QRS complexes. Especially since heartbeats that belong to Ventricular ectopic beat(VEB) are initiated by ectopic focuses in ventricles instead of the sinoatrial node, the reverse depolarization process could generate various QRS complex morphologies. For example, nearly half of the 48 recordings of MIT-BIH Arrhythmia Database have multiform Premature ventricular contractions(PVC). This makes classifiers modeled by machine learning techniques uneasy to work when they meet new patients. Patient-dependent design is a promising method to mitigate the problem, and has been achieved by several researchers. For instance, Hu et.al [24] combined a global classifier with a local classifier through a mixture of experts approach(MOE), the global classifier was designed from a large database of labeled ECG data, and the local classifier was trained by patient dependent data; Chazal et.al [25] and Alexander et.al [12] also combine the global classifier and local classifier that are realized by linear discriminant analysis (LDA) technique; Ince et.al [13] proposed a multi-dimensional particle swarm optimization technique and trained with small amount of common and patient-specific data; Li et.al [10]

proposed a parallel general regression neural network (GRNN) and used half of the randomly chosen data as training data and the other half data for testing; Kiranyaz et.al [26] proposed an 1-D convolutional neural networks and trained with 245 common beats and a first 5 minutes of each patient data. These researches have shown that the patient-dependent designs have the ability to improve classification accuracy. Therefore, our proposed parallel Delta modulation based machine learning system also integrate the combination of global classification and local classification for patient-specific training.

To evaluate the performance of our proposed system, we used the MIT-BIH Arrhythmia Database [27], [28], which includes 48 records. Each record has two channels and both of the channels are fully annotated with 30 minutes duration. Most records in MIT-BIH Arrhythmia Database have one channel ECG data from the modified limb lead II (MLII), while the other channel may come from the modified leads V1, V2, V4 or V5. Data from MLII is used in this paper. All data from the MIT-BIH Arrhythmia Database has already been processed by a passband filter from 0.1 to 100 Hz. Though there are still a number of artifacts such as baseline wondering, electromyographic noise and motion that influence the quality of the signals, we decide to feed original data from this database directly into our system, so that the signal quality meets practical scenarios of wearable ECG monitoring sensors.

Heartbeats from the MIT-BIH Arrhythmia database are classified into 20 classes. According to the Advancement of Medical Instrumentation(AAMI) standard [19], these 20 types are relabeled into 5 classes: N for beats originating in the sinus node, S for Supraventricular ectopic beats (SVEB), V for VEB, F for fusion beats and Q for unknown beats. The classifications of S and V are used to evaluate the performance of the proposed algorithm. The SVEB data include beats labeled as Atrial premature beat, Aberrated atrial premature beat, Nodal (junctional) premature beat and Supraventricular premature beat in the MIT-BIH database. The VEB data contain PVC and Ventricular escape beats.

For patient specific design, according to [12] and [25], the recordings of the MIT-BIH Arrhythmia database are divided into two groups, the training data group (Tg): 101, 106, 108, 109, 112, 114, 115, 116, 118, 119, 122, 124, 201, 203, 205, 207, 208, 209, 215, 220, 223, 230, and the inference data group (Ig): 100, 103, 105, 111, 113, 117, 121, 123, 200, 202, 210, 212, 213, 214, 219, 221, 222, 228, 231, 232, 233, 234. The first 500 beats of each recording in Ig plus a basis dataset are selected to train the according local classifiers while all data in Tg are selected for training the global classifier, then the rest data of each recording in Ig are used for inference to evaluate the proposed classifier and the performance of the system. The classification tasks are distinguishing V versus the rest four classes (N, S, F, Q) and S versus the rest classes (N, V, F, Q), which are two binary classification tasks.

III. Parallel Delta Modulators and QRS/PT Detection

QRS complex detection is one of the most important parts in wearable ECG monitoring sensor design. There have been several QRS complex detection algorithms proposed in the past, which can be categorized in two types. The first type uses wavelet transforms [29], or artificial neural networks [30], which utilized CPU or DSP to achieve very accurate detection results. The second type applies on-chip cross-correlation [31], pulse triggered and time-assisted pulse triggered [32], integrate and fire pulse train automaton [33], or input-feature correlated algorithm [34], which have the samplers combining analog to digital converter (ADC) and data processing to achieve reasonably precise results with low hardware cost. In our proposed system, we use a sub-micro watts paralleled Delta modulator based sampler [20] that follows the second type strategy.

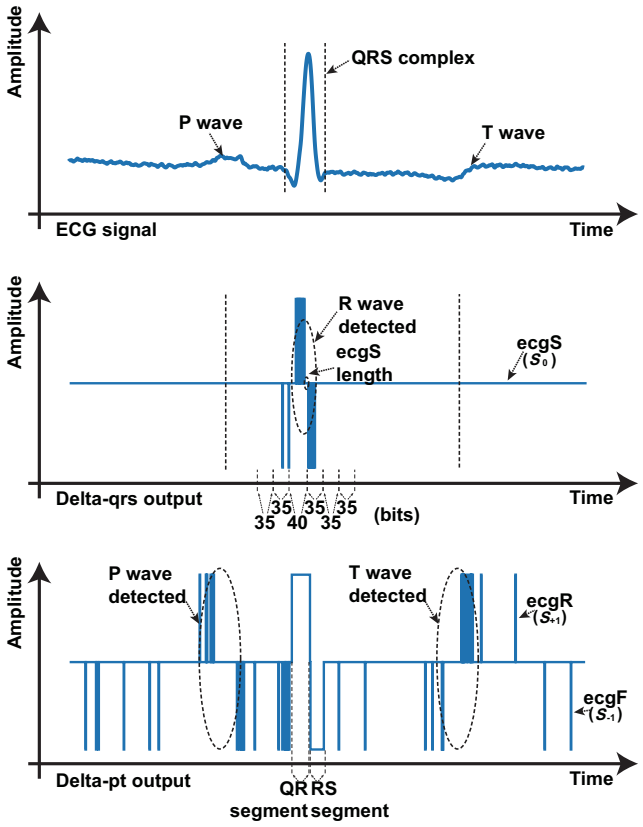

Fig. 3. Parallel Delta modulation of ECG data (Record 100). Top: Input ECG waveform. Middle: Delta-qrs output to detect R wave, where ecgS length measures the duration of the R peak. Features are extracted from the six segments of the bit-stream. Bottom: Delta-pt output to detect P wave and T wave, where QR and RS segment are measured.

The parallel delta modulator is shown in Fig. 1. Two first-order three-state Delta modulators ($Delta-qrs$ and $Delta-pt$) with the following QRS and PT detection algorithms are used to detect QRS and PT waves separately. In the system, the PT detection algorithm obtains information of the detected R peak from the QRS detection algorithm in order to locate P and T waves. $Delta-qrs$ and $Delta-pt$ are both three-state Delta modulators with different trigger reference voltages and integration gains. Lower trigger reference voltage and

integration gain make $Delta - pt$ sensitive to low amplitude variations of the ECG signal, that includes P, T, and U waves which will be neglected by $Delta - qrs$. This also makes $Delta - pt$ easily saturate in processing large amplitude waves such as R waves. The input ECG signal V_{in} subtracts the integrated feedback voltage V_{fb} to generate the delta voltage V_d. Then V_d is compared with the trigger reference voltages $+V_{ref}$ and $-V_{ref}$. The comparison has three potential results, i.e., three states: S_{+1}, S_0, and S_{-1}. Here S_{+1} indicates the input signal is rising, which is labeled as $ecgR$. Similarly, S_{-1} means the input signal is falling and labeled as $ecgF$. S_0 means V_d is between the window formed by $+V_{ref}$ and $-V_{ref}$, it is labeled as $ecgS$. Denser $ecgR$s mean the input signal is rising with a higher slope, and vice versa. A long period of time of $ecgS$ means the input signal stays in the range of $\pm V_{ref}$. An example of the Delta modulator output with an ECG signal input is shown in Fig. 3.

The parallel Delta modulated bit-streams provide slope information of both the QRS complex and P/T waves. In [20], we proposed the Local Maximum Point (LMaP) and Local Minimum Point (LMiP) algorithms to process the Delta modulated bit-streams in order to detect the location of the QRS complex, as well as the P waves and T waves. Here we briefly summarize the algorithm. The LMaP or LMiP algorithm counts the number of consecutive $ecgR$ or $ecgF$ labels in the bit-streams, and compare the number with a pre-defined threshold value to detect a real rising or falling slope. On the other hand, the LMaP or LMiP algorithm includes a protection mechanism: if the duration between the $ecgR$ or $ecgF$ labels is more than a pre-defined value, the algorithm resets the detection process. Therefore, both slow variations and low amplitude variations in the waveforms do not trigger the QRS and PT detection process. Moreover, the QRS and PT detection process can help each other by exchanging the detection processing status and timing information. A more detailed description of the algorithm can be found in our previous paper [20]. Since the LMaP/LMiP algorithm is based on counters, which is more power efficient than arithmetic operations, the system can perform real-time processing on the sensor hardware.

IV. Patient-dependent rotation SVM Classification

A. Feature Extraction

Features used in this study mainly focus on the morphology of QRS complexes. The features should be easily extracted from the Delta modulated bit-stream using a counter based method, which avoids power hungry computation functions. In the proposed system, once an R wave peak is identified, the QRS detection algorithm sends two 215 ms length bit-streams in the local memory for feature extraction, one from $Delta - qrs$ and the other from $Delta - pt$. Since the Delta modulator is working at 1K sample/second, a 215 ms bit-steam means 215 bits. The bit-stream from $Delta - qrs$ is divided into six segments. As shown in Fig. 3, among the six segments, three 35 bit segments are after the R peak, while two 35 bit and one 40 bit segments are before the R peak. The selected features are then extracted from each segment. The feature vector are designed as follows:

1) Skewness weight. The skewness weights are calculated by the number of $ecgR$ and $ecgF$ events in each of the six segments. So there are total twelve skewness weight values from a 215 bit $Delta - qrs$ bit-stream. When calculating the skewness weight, a solitary $ecgR$ relates to added weight of 1. If there are consecutive $ecgR$ events, the latter added weight doubles and the maximum is set to 8. For example, in calculating the skewness weight of a bit-stream '0100111110', the skewness weight equals to '0+1+0+0+1+2+4+8+8+0', which is 24. Skewness weight of $ecgF$ is calculated in the same method.

2) $ecgR$ and $ecgF$ events. The number of $ecgR$ and $ecgF$ events in each segment. There are total twelve values, six for $ecgR$ events and six for $ecgF$ events from a 215 bit $Delta - qrs$ bit-stream.

3) R wave polarity, $ecgS$ length, and QR/RS length. R wave polarity is obtained from the first bit of the 35-bit data right after R peak. $ecgS$ length is calculated by counting the number of zeros in the first consecutive zero bit stream section from the 40-bit segment in a reverse order. The QR and RS length are calculated by counting the maximum length of continuous $ecgR$ and $ecgF$ respectively in the 215-bit data from $Delta - pt$ if the R peak polarity is positive, otherwise by counting that of $ecgF$ and $ecgR$, respectively.

4) RR intervals, P/T wave polarities.* Pre-RR interval, Post-RR interval and polarities of P and T waves can be obtained using our previously proposed algorithm in [20], which are applied as extra feature values.

Three types of feature vectors are applied in this paper for classification: SkW-28 includes 28 feature values of (1)-(3), SkR-30 includes SkW-28 and the Pre-RR and Post-RR intervals, and SkP-32 includes all features (1)-(4*).

B. SVM Hyperplane Rotation

Many classifiers have been proposed for Arrhythmia classification. Beside previously mentioned LDA classifier [12], [35], parallel general regression neural network [10], 1-D convolutional neural networks [26], and ANN with multidimensional particle swarm optimization(MD PSO) technique [13], there are also Block-Based Neural Networks [36], linear discriminant classifier with feature extracted from discrete wavelet transform [37], and SVM classifiers [11], [38]–[40]. Among these classifiers, SVM has been broadly used to solve practical classification problems due to its excellent generalization ability. However, SVM's hardware implementation cost depends on its kernel function. A practical SVM classifier [41] shows that the classifier with kernel function of radical basis function (RBF) costs more than 50000 times power consumption per classification compared to a linear kernel function. Therefore, SVM classifiers with kernel function of RBF [11], [38]–[40] may not be suitable for wearable ECG sensors. Also, if implemented on integrated circuits, the features extraction process using wavelet transform [11] is also power hungry. Thus, in this paper, a linear kernel is

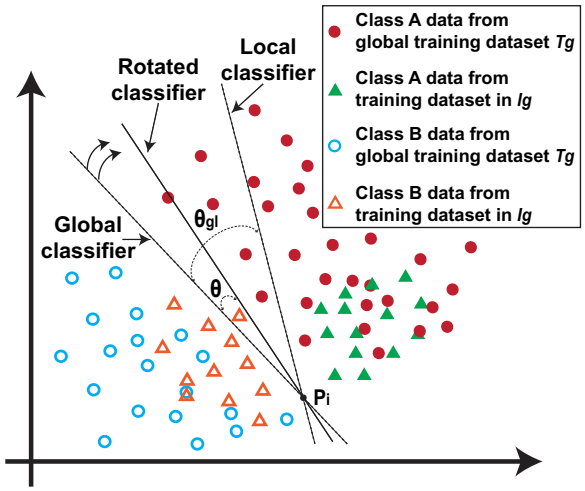

Fig. 4. The proposed patient-specific rotated classifier rotated between the local classifier and the global classifier. Circular marks represent data from training group Tg, and triangular marks represent data from patient dependent dataset of each record in inference group Ig. Solid marked data belongs to class A, while hollow marked data belongs to class B.

implemented by rotating the global classifier to a certain angle to obtain a patient dependent SVM classifier.

We apply a similar strategy described in [12] to achieve the patient dependent classification. In [12], the author used LDA method and defined a parameter that weighs the local and global classifiers. In this paper, based on features extracted from the Delta modulated bit-stream, we introduce an angle θ to rotate the global SVM classification hyperplane. The local and global SVM classifiers are implemented through LIBSVM library [42].

A simplified explanation of the proposed hyperplane rotation method is illustrated in Fig. 4, where a two dimensional feature vector and two classes (class A and class B) are used as an example. The global classifier decision boundary is formed by training all the data from Tg, and the local classifier is trained by the patient dependent dataset including the first 500 samples from each record in Ig and a basis dataset. Let θ_{gl} to be the angle between the global and local decision boundary. Since a linear kernel function is applied, the global and local decision boundaries are two one dimension lines that has an inter section point. We use a parameter K_k that weighs the rotation angle. K_k is defined in relation to the number of samples in a given class as in [12] and [25]:

$$K_k = \max\left\{1 - \frac{N_k^g}{10}, 1 - W\right\} \tag{1}$$

where N_k^g is the number of samples in class k and the parameter W is usually set to 0.7. Thus the global hyperplane pivots the intersection point P_i with an angle $\theta = K_k \cdot \theta_{gl}$ to the direction as shown in Fig. 4, the formed new boundary is the patient dependent decision boundary.

Unlike in [12], in the case that a certain heartbeat class may not be included in the local training set due to the limited data volume (which make the local classifier invalid), records 209 and 215 are selected to be added into local classifier's training dataset as the basis dataset, plus the patient dependent training set (500 samples), the local classifier could be trained. Since even if there is only one class in the patient dependent training set, it includes useful information to form the classification boundary. In the following, we present the process of combining the two classifiers.

As stated above, we use data from Tg to train the global classifier $F_{global}(x) = 0$, where

$$F_{global}(x) = \sum_{i=1}^{N} w_{gi}x_i + b_{g0} \tag{2}$$

Also, we can find the local classifier $F_{local}(x) = 0$ in training with the 500 samples of each record in Ig (including record 209 and 215 as basis):

$$F_{local}(x) = \sum_{i=1}^{N} w_{li}x_i + b_{l0} \tag{3}$$

To combine the global and local classifiers, we rotate the hyperplane defined by the global classifier towards the hyperplane defined by the local classifier for θ degrees, around the $N-1$ dimension intersection hyperplane of the two classifiers, and the rotated hyperplane is the new classification boundary. Before we proceed to find the new classifier, we introduce several notations and a general assumption. First, define $\vec{n_g} = (w_{g1}, w_{g2}, \cdots, w_{gn})$ and $\vec{n_l} = (w_{l1}, w_{l2}, \cdots, w_{ln})$ as the normal vectors of hyperplane F_{global} and F_{local}, respectively. Then assume that the inner product of $\vec{n_g}$ and $\vec{n_l}$ are positive, denoted as $\langle \vec{n_g}, \vec{n_l} \rangle > 0$. Otherwise, let $\vec{n_g} = (-w_{g1}, -w_{g2}, \cdots, -w_{gn})$ instead. Without losing of generality, we assume that

$$w_{g1}w_{l2} - w_{g2}w_{l1} \neq 0 \tag{4}$$

To find the exact expression of the new classifier, we use the following three steps.

At first, we define a linear equation system

$$\begin{cases} \sum_{i=1}^{N} w_{gi}x_i + b_{g0} = 0 \\ \sum_{i=1}^{N} w_{li}x_i + b_{l0} = 0 \end{cases} \tag{5}$$

and find a special solution of the above equation system. From the assumption there are infinite solutions when $N > 2$. Here we choose the special solution $\xi_0 = (x_1^0, x_2^0, 0, \cdots, 0)$ where

$$x_1^0 = \frac{w_{g2}b_{l0} - w_{l2}b_{g0}}{w_{g1}w_{l2} - w_{g2}w_{l1}} \tag{6}$$

$$x_2^0 = \frac{w_{l1}b_{g0} - w_{g1}b_{l0}}{w_{g1}w_{l2} - w_{g2}w_{l1}} \tag{7}$$

In the second step, we define the normal vectors of a family of hyperplanes between the hyperplane defined by $F_{global}(x) = 0$ and $F_{local}(x) = 0$. Let

$$\vec{n_t} = [(1-t)\vec{n_g} + t\vec{n_l}] \tag{8}$$

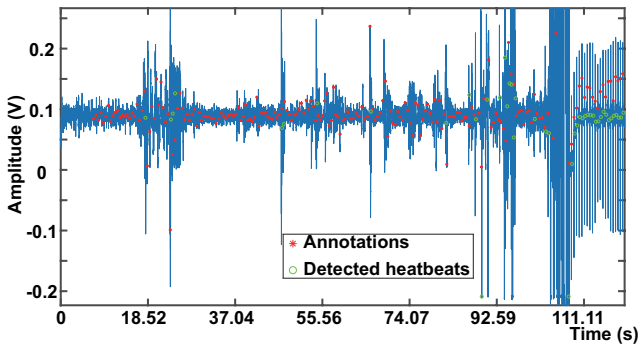

Fig. 5. Noise filled part of record 2800, FN and FP increase.

For $t \in (0, 1)$. We solve the solution $\vec{n_t}^* \in \vec{n_t}$ with equation

$$\arccos\left(\frac{\left\langle \vec{n_g}, \vec{n_t^*} \right\rangle}{|\vec{n_g}| \cdot \left|\vec{n_t^*}\right|}\right) = \theta \tag{9}$$

where $\theta = K_k \cdot \theta_{gl}$ and θ_{gl} is the angle between F_{global} and F_{local} and is calculated by

$$\theta_{gl} = \arccos\left(\frac{\langle \vec{n_g}, \vec{n_l} \rangle}{|\vec{n_g}| \cdot |\vec{n_l}|}\right) \tag{10}$$

Finally, we reach the desired classifier

$$F_{rotate}(x) = \sum_{i=1}^{N} w_{ri} x_i + b_{r0} \tag{11}$$

by solving the equation

$$\left\langle \vec{n_t^*}, x - \vec{\xi}_0 \right\rangle = 0 \tag{12}$$

The rotated classifier defines a classification hyperplane for any fixed angle of θ. When $\theta = 0$, the hyperplane is defined by $F_{global}(x) = 0$, and it is defined by $F_{local}(x) = 0$ when $\theta = \theta_{gl}$, and for $\theta \in [0, \theta_{gl}]$, the hyperplane stays in the between.

V. Results

A. Performance evaluation

Since the proposed system is targeted on wearable application, the QRS detection algorithm is evaluated by both the MIT-BIH Arrhythmia database and another noisy database used for the PhysioNet/Computing in Cardiology Challenge 2014 [43], the Robust Detection of Heart Beats in Multimodal Data(RDHBMD). Following [20] we modified our algorithm by using a more stringent rule for detecting QRS complexes, which aims at collecting more stable and uniform data for heatbeats classification, and all performances are shown in Table. I including both the previously reported algorithm and the modified one using the MIT-BIH database. The four paced recordings (102, 104, 107 and 217) that are not included in Tg and Ig are also included to evaluate the QRS detection performance. The New Augmented Training Set in RDHBMD(RDHBMD-NATS) is much noisier than the Training Set(RDHBMD-TS), both datasets include 100 10-min ECG recordings. Some recordings in RDHBMD-NATS contain lots of noise that the heartbeats could not be identified by ECG signal like part of the record 2283 and 2800 as shown in Fig. 5. Some recordings lose ECG information for part of the recording like record 1522 and 1715, and record 42878 does not have ECG signal at all. Those heartbeats annotations could only be defined by other associated information in the database, such as blood pressure, photoplethysmograms, etc. Overall the proposed algorithm could get sensitivity value for over 91% and positive predictive value for over 95%, which are defined in the following paragraph.

TABLE I
Heartbeats detection results by the proposed QRS detection algorithm

Database	Total Beats	FN	FP	SE	PPV
MIT-BIH	109966	911	494	99.17	99.55
RDHBMD-TS	72416	392	416	99.46	99.43
RDHBMD-NATS	78622	6387	3399	91.88	95.51
MIT-BIH(modified)	109966	1556	669	98.59	99.39

The performance of the proposed heartbeats classification system is evaluated using the collected data from the modified QRS detection algorithm of [20] in MIT-BIH Arrhythmia Database with AAMI standard. Five parameters: F1 score(*F1*), accuracy(*ACC*), sensitivity(*SE*), specificity(*SP*) and positive predictive value(*PPV*) are used to evaluate the performance of the algorithm, which are defined as follows:

$$F1 = \frac{2 \times TP}{2 \times TP + FP + FN} \tag{13}$$

$$ACC(\%) = \frac{TN + TP}{TN + TP + FN + FP} \tag{14}$$

$$SE(\%) = \frac{TP}{TP + FN} \tag{15}$$

$$SP(\%) = \frac{TN}{TN + FP} \tag{16}$$

$$PPV(\%) = \frac{TP}{TP + FP} \tag{17}$$

where TP, TN, FP and FN represent true positive, true negative, false positive and false negative classifications, respectively. The 22-fold recording-by-recording cross validation method proposed in [25] is applied to Tg, for assessing the classifier performance and finding the optimum W. The folds were split into training data that includes 21 folds with each fold containing one recording, and test data containing data from the remaining fold(recording). The average results of this recording-by-recording cross validation on Tg are reported in Table. III. The global classifier was trained on training data and local classifier was trained on the first 500 beats of the test data. The classifier performance was assessed on the remaining beats of the test recording. With the W the detailed evaluation on Ig is reported in Table. II. Since the data used for evaluation are collected by the modified QRS

TABLE II
CLASSIFICATION RESULTS USING THE SKP-32 FEATURE VECTORS FOR EACH OF THE TEST PATIENTS

	Number of Beats				Number of Beats Detected					SVEB					VEB				
REQ	N	S	V	F+Q	N	S	V	F+Q	FP	F1	ACC	SE	PPV	SP	F1	ACC	SE	PPV	SP
100	1744	28	1	0	1741	28	1	0	1	1	100.00	100.00	100.00	100.00	0	99.89	0.00	0.00	99.94
103	1582	2	0	0	1580	2	0	0	0	0	99.87	0.00	100.00	-	-	100.00	-	-	100.00
105	2041	0	26	5	1963	0	26	3	144	0	99.53	-	99.53	0.00	0	95.46	0.00	0.00	96.64
111	1623	0	1	0	1613	0	1	0	7	-	100.00	-	100.00	-	0	99.81	0.00	0.00	99.88
113	1293	2	0	0	1289	2	0	0	0	1	100.00	100.00	100.00	100.00	-	100.00	-	-	100.00
117	1034	1	0	0	1029	1	0	0	1	0	99.90	0.00	100.00	-	-	100.00	-	-	100.00
121	1361	1	1	0	1351	1	1	0	3	0	99.93	0.00	100.00	-	0	99.93	0.00	-	100.00
123	1016	0	2	0	1014	0	2	0	0	-	100.00	-	100.00	-	0.67	99.90	50.00	100.00	100.00
200	1390	28	681	2	1385	28	677	1	36	0	97.32	0.00	98.62	0.00	0.97	98.07	95.42	98.48	99.31
202	1569	54	12	1	1559	49	1	1	0	0.58	97.45	57.14	98.72	58.33	0	99.94	0.00	-	100.00
210	1959	20	162	9	1924	15	142	7	4	0.63	99.38	73.33	99.57	55.00	0.89	98.66	83.80	95.97	99.74
212	2248	0	0	0	2239	0	0	0	4	0	99.96	-	99.96	0.00	0	99.96	-	0.00	99.96
213	2252	27	199	273	2247	27	195	269	0	0.93	99.85	92.59	99.93	92.59	0.87	97.99	91.28	82.41	98.51
214	1564	0	197	1	1555	0	197	1	0	-	100.00	-	100.00	-	0.72	93.90	71.57	73.44	96.72
219	1604	3	47	0	1602	3	47	0	0	0	99.82	0.00	100.00	-	0.89	99.46	80.85	100.00	100.00
221	1626	0	301	0	1622	0	296	0	0	-	100.00	-	100.00	-	0.99	99.84	98.99	100.00	100.00
222	1774	209	0	0	1695	209	0	0	8	0.21	89.59	12.44	99.06	61.90	0	99.53	-	0.00	99.53
228	1300	3	250	0	1283	3	247	0	50	0	98.74	0.00	98.92	0.00	0.95	98.29	97.98	91.67	98.35
231	1071	0	0	0	1065	0	0	0	0	-	100.00	-	100.00	-	-	100.00	-	-	100.00
232	271	1009	0	0	270	1006	0	0	10	0.96	94.01	97.12	82.86	95.32	0	99.69	-	0.00	99.69
233	1873	4	696	6	1869	4	696	6	0	0	99.84	0.00	100.00	-	0.99	99.65	98.85	99.85	99.95
234	2200	50	3	0	2198	50	3	0	0	0.82	99.33	70.00	100.00	100.00	1	100.00	100.00	100.00	100.00

detection algorithm, the classifier is not able to be evaluated by those missed heartbeats(part of the FNs in Table. I, including 302 missed N beats, 13 missed S beats, 47 missed V beats, 7 missed F beats and 2 missed Q beats). Moreover, 268 FP beats are taken into classification as shown in Table. II. Thus in practice, the two classification tasks are performed as S versus N, V, F, Q and FP beats, and V versus N, S, F, Q and FP beats, respectively. The Average classification performances compared with other published state-of-the-art literatures are reported in Table. III.

From Table. III the proposed methods is at the same level of the best performance among the references. Compared to [12], [13], [24]–[26], the proposed SkW-28 has better performance in classifying SVEB, while SkR-30 and SkW-32 have medium *SE* value(less than 10% compared to the best) but better *PPV* and *F1* score. For classifying VEB, [25] has the best *SE* value(94.3%), *PPV*(96.2%) and *F1* score(0.95) that are 1.5%(1.6%), 4.6% and 0.03 better than SkP-32(SkR-30), respectively, with SP at the same level, and are 4.2%, 4.2%, and 0.04 better than SkW-28. Above all we note that [26] used only a tiny amount of data for training both the global and local classifiers to achieve such good results. [10] achieved 92.3% *PPV* in distinguishing SVEB that is 9.9%, 6.3%, 4.1% better than our proposed method SkW-28, SkR-30, SkP-32, respectively. However, [10] is not targeted on wearable-device applications and GRNN is a GPU-based algorithm, while our proposed SVM classifier with linear kernel needs only 28-32 multiplications and 29-33 additions to complete a classification, which is more friendly to low power circuit design.

TABLE III
AVERAGE CLASSIFICATION RESULTS COMPARED TO THE STATE OF ART

Methods	SVEB					VEB				
	F1	ACC	SE	SP	PPV	F1	ACC	SE	SP	PPV
Hu et.al [24]	0.80	95.5	82.6	97.1	77.7	-	-	-	-	-
Ince et.al [13]	0.58	97.4	63.5	99.0	53.7	0.86	98.3	84.6	98.7	87.4
Chazal et.al [25]	0.61	95.9	87.7	96.2	47.0	0.95	99.4	94.3	99.7	96.2
Alexander et.al [12]	0.68	-	86.2	97.5	56.7	0.94	-	92.4	99.6	94.8
Li et.al [10]	0.89	99.4	85.5	99.4	92.3	0.90	98.9	88.0	98.9	92.6
Kiranyaz et.al [26]	0.62	97.6	60.3	99.2	63.5	0.92	99.0	93.9	98.9	90.6
Proposed SkW-28	**0.86**	**98.9**	**90.0**	**99.3**	**82.4**	**0.91**	**98.8**	**90.1**	**99.4**	**92.0**
Proposed SkR-30	0.82	98.7	78.5	99.5	86.0	0.92	99.0	92.7	99.4	91.6
Proposed SkP-32	0.83	98.8	79.3	99.6	88.2	0.92	99.0	92.8	99.4	91.6
Proposed SkW-28[a]	0.84	98.9	88.3	99.2	79.7	0.91	98.8	90.1	99.4	92.3
Proposed SkR-30[a]	0.89	99.2	91.0	99.5	86.8	0.92	98.9	92.7	99.4	91.9
Proposed SkP-32[a]	**0.90**	**99.3**	**90.7**	**99.6**	**89.0**	**0.92**	**98.9**	**92.8**	**99.4**	**91.9**
Proposed SkW-28[b]	**0.87**	**99.0**	**92.4**	**99.2**	**82.4**	**0.91**	**98.8**	**90.1**	**99.4**	**92.0**
Proposed SkR-30[b]	0.84	98.8	80.0	99.6	88.3	0.92	98.9	92.7	99.4	91.6
Proposed SkP-32[b]	0.84	98.9	80.1	99.6	89.3	0.92	98.9	92.8	99.4	91.6
Proposed SkW-28[c]	0.47	98.0	45.5	99.0	48.7	0.82	99.5	85.3	98.2	78.4
Proposed SkR-30[c]	0.82	99.3	84.3	99.6	80.5	0.82	94.7	86.4	98.0	77.7
Proposed SkP-32[c]	**0.84**	**99.3**	**86.8**	**99.6**	**80.6**	**0.82**	**97.2**	**86.5**	**98.1**	**77.9**
Proposed SkW-28[d]	0.36	97.6	35.1	98.8	37.7	0.81	96.8	86.8	97.8	75.9
Proposed SkR-30[d]	0.81	99.2	88.2	99.4	74.4	0.81	97.1	87.4	97.8	76.0
Proposed SkP-32[d]	**0.81**	**99.2**	**88.6**	**99.4**	**73.9**	**0.82**	**97.1**	**87.5**	**97.9**	**76.3**
Proposed SkW-28[e]	0.77	98.0	89.2	98.3	67.4	0.85	97.9	88.5	98.5	81.3
Proposed SkR-30[e]	0.72	97.8	77.8	98.5	67.5	0.86	98.0	91.0	98.5	81.3
Proposed SkP-32[e]	**0.73**	**97.9**	**78.6**	**98.6**	**68.9**	**0.86**	**98.0**	**91.1**	**98.5**	**81.3**

[a] Averaged evaluation results without record 222.
[b] Averaged evaluation results without record 202.
[c] Reverse dataset evaluation results.
[d] 22-fold Cross-validation results.
[e] Worst case scenario results.

B. Discussions

The performance of proposed SkW-28 is better than SkR-30 and SkP-32 mainly because of record 222. Record 222 has a very large amplitude variation as shown in Fig. 6, some heart beats with very small amplitude may result in missing recognition of QRS detection algorithm, the average amplitude of R wave peak in region 1 is two or three times larger than that in region 2 as shown in bottom panel of Fig. 6. The large amplitude variation caused missing QRS detections makes the feature vector of the next identified heart beat a large pre-RR interval value and the previous feature vector

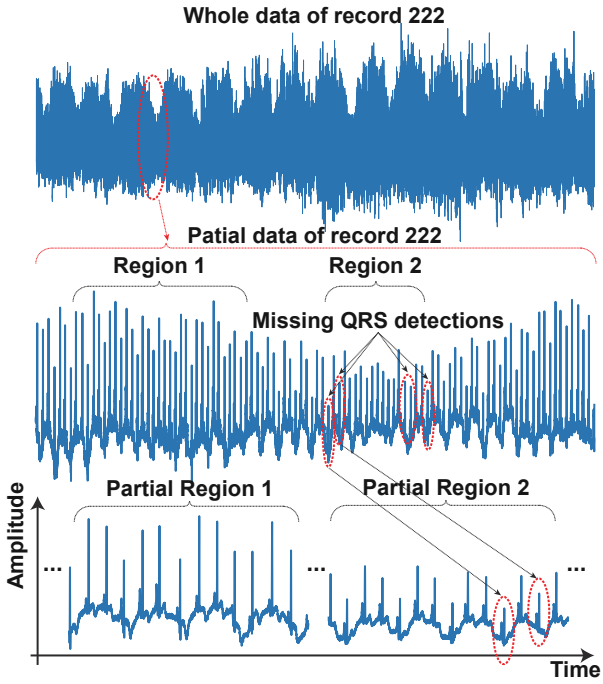

Fig. 6. Large amplitude variation in record 222 caused missing QRS detections which make pre/post-RR interval irregular. Top: the whole ECG waveform of record 222. Middle: ECG waveform of the large amplitude variation part of record 222. Bottom: detailed ECG waveform that showing small amplitude QRS complexes which caused missing detection.

a large post-RR interval value, which becomes features of irregular heart beats thus brings confusion to classifiers. The advantages of adding RR intervals as elements of feature vectors then become disadvantages. Table. III also shows the performance of the proposed method without record 222. Overall, SkP-32 has better performance if there are no large amplitude variations in ECG signals under test. By analyzing the evaluation results of global, local and the rotated classifiers, we also found that in all global classifiers, global classifier of SkP-32 has best performance. SkW-28's local classifier of record 222 performs much better than the others, which is a big help for its final best results. Overall, patient rotated classifiers bring obvious *SE* improvements compared with using global classifiers only. Taking advantages of the proposed technique, 43%, 19%, and 18% of *SE* value of SkW-28, SkR-30 and SkP-32 are enhanced in classifying SVEB compared with using global classifiers only, respectively, and 38%, 36% and 36% for classifying VEB, respectively. *PPV* of SkW-28 in classifying SVEB improves 14% while *PPV* of SkR-30 and SkP-32 deduct 5% and 2%, respectively. *ACC* and *SP* values have no distinct improvement or degradation.

Moreover, record 201 and 202 come from the same patient, but are splitted into Tg and Ig, so we also include the results without record 202 in Table. III. The results show that it does not affect the performance.

Another potential issue is that such splitting the dataset into Tg and Ig may cause selection bias, so we run a reverse evaluation, i.e., trained with Ig and test with Tg, the results are also included in Table. III. The results show that such splitting dataset will cause selection bias and affect SkW-28 method in classifying SVEB. SE and PPV value reduced to below 50%. However, it has little influence on detecting VEB or on SkR-30 and SkP-32. By analyzing each patient's ECG signal, one possible reason of decadence of SkW-28 is that the morphological difference of SVEB in *Ig* is more distinct than that in *Tg*, like record 222 and record 232 that contain large amount of SVEBs, while in record 209 of *Tg*, only a small amount of SVEBs have recognizable morphological difference, and could be classified by SkW-28. Moreover, in record 220 and 223, one can hardly tell the difference between a normal heartbeat and an SVEB without considering RR interval difference or P/T waves, thus SkW-28 fails to work. Though the results show that such splitting dataset causes selection bias for SkW-28 method, this method is effective especially in processing ECG signals like record 222. Also [44] expressed concern that such patient dependent classification scheme is not a realistic performance measure of automatic heartbeat classification, and it leads to optimistic results for less interpatient ECG characteristics variation. We have to admit the limitation of the universal applicability of such patient-adapting researches [10], [12], [13], [24]–[26], so we proposed a future realistic customization based application situation as shown in Fig. 2, to overcome this limitation and take advantage of obviously improved classification performance by sacrificing cost of data transmission and labor force in base station.

The missed heartbeats is a shortcoming in the evaluation process of the proposed classifier. To compare with other published researches, we consider the worst case scenarios that (1) all missed N, V, F, and Q beats are FP in classifying SVEB; (2) all missed N, S, F, and Q beats are FP in classifying VEB; (3) all missed S beats are FN in classifying SVEB; and (4) all missed V beats are FN in classifying VEB. The results of the worst case scenarios are also shown in Table. III. In the worst case scenarios, the performance of the preferred SkP-32 in classifying SVEB is still comparable to other researches, but the PPV of classifying VEB reduces around 10% and is worse than others. However, since only a small amount of S and V beats are missed (0.9% for S and 1.8% for V), the *SE* values has not changed much by the missed heartbeats.

In the future work, one possible solution of improving the performance of the system is to modify the QRS detection algorithm [20], making an alert signal when detecting a prolonged RR interval. At the meantime, an R peak value detection block can be included in the front analog circuits [23] to identify if there is large variation in amplitude like record 222, so that the classifier to switch to a better feature option. The proposed system could detect heartbeats in a medium noise infected ECG signal, for noise signal that has morphology and location similar to the real QRS complex, or severe baseline drift, the system needs extra assistance, and a well designed band-pass filter in analog front end circuits [45] may be a solution.

VI. Conclusion

This paper describes a real-time ECG processing algorithm to classify two Arrhythmic heartbeats with AAMI standard. The proposed method is based on low-power parallel Delta modulators and targeting for low computing overhead on-sensor machine learning systems. The overall system contains the parallel Delta modulator as the sampler and the following QRS detection algorithm, as well as the patient dependent linear-kernel SVM classifier with feature vectors extracted directly from the output of the sampler. The proposed patient dependent classifier is formed by rotating of the global classifier around the intersection hyperplane with the local classifier to a certain angle. The performance of the classifier is evaluated on F1 score, sensitivity, specificity and positive prediction values through the MIT-BIH Arrhythmia database, and the results show that in classifying SVEB, our proposed and preferred method SKP-32 could reach 0.83, 79.3%, 99.6% and 88.2% for the four metrics, respectively, and 0.92, 92.8%, 99.4% and 91.6% for VEB classification, respectively, which is at the same level of those best classifiers in the published researches. SkR-28 method is susceptible to selection bias, but is effective especially in processing data like record 222 in the database. With future modification of the according algorithm and assistance from other circuits, SkR-28 may play important role in some cases. Since the sampler presented in [20] is a sub-micro watts implementation, and the proposed classifier in this paper is based on a linear kernel function, the inference only take 28-32 multiplications and 29-33 additions based on different type of feature vectors. Therefore, the proposed system is very promising in future low power wearable ECG monitoring sensors with real time on-site signal processing applications.

References

[1] "New initiative launched to tackle cardiovascular disease, the world's number one killer." [Online]. Available: http://www.who.int/cardiovascular_diseases/en/

[2] E. J. Benjamin, S. S. Virani, C. W. Callaway, A. M. Chamberlain, A. R. Chang, S. Cheng, S. E. Chiuve, M. Cushman, F. N. Delling, R. Deo *et al.*, "Heart disease and stroke statistics—2018 update: a report from the American Heart Association," *Circulation*, vol. 137, no. 12, pp. e67–e492, 2018.

[3] H. C. McGill Jr, C. A. McMahan, and S. S. Gidding, "Preventing heart disease in the 21st century: implications of the Pathobiological Determinants of Atherosclerosis in Youth (PDAY) study," *Circulation*, vol. 117, no. 9, pp. 1216–1227, 2008.

[4] X. Zhang, Z. Zhang, Y. Li, C. Liu, Y. X. Guo, and Y. Lian, "A 2.89-μ W Dry-Electrode Enabled Clockless Wireless ECG SoC for Wearable Applications," *IEEE journal of solid-state circuits*, vol. 51, no. 10, pp. 2287–2298, 2016.

[5] D. Da He and C. G. Sodini, "A 58 nW ECG ASIC with motion-tolerant heartbeat timing extraction for wearable cardiovascular monitoring," *IEEE transactions on biomedical circuits and systems*, vol. 9, no. 3, pp. 370–376, 2015.

[6] C.-I. Ieong, P.-I. Mak, C.-P. Lam, C. Dong, M.-I. Vai, P.-U. Mak, S.-H. Pun, F. Wan, and R. P. Martins, "A 0.83-QRS detection processor using quadratic spline wavelet transform for wireless ECG acquisition in 0.35-CMOS," *IEEE Trans. Biomed. Circuits Syst*, vol. 6, no. 6, pp. 586–595, 2012.

[7] Y. Chuo, M. Marzencki, B. Hung, C. Jaggernauth, K. Tavakolian, P. Lin, and B. Kaminska, "Mechanically flexible wireless multisensor platform for human physical activity and vitals monitoring," *IEEE transactions on biomedical circuits and systems*, vol. 4, no. 5, pp. 281–294, 2010.

[8] V. Sze, Y.-H. Chen, J. Emer, A. Suleiman, and Z. Zhang, "Hardware for machine learning: Challenges and opportunities," in *Custom Integrated Circuits Conference (CICC), 2018 IEEE*, pp. 1–8.

[9] S. Raj and K. C. Ray, "ECG signal analysis using DCT-based DOST and PSO optimized SVM," *IEEE Transactions on Instrumentation and Measurement*, vol. 66, no. 3, pp. 470–478, 2017.

[10] P. Li, Y. Wang, J. He, L. Wang, Y. Tian, T.-s. Zhou, T. Li, and J.-s. Li, "High-performance personalized heartbeat classification model for long-term ECG signal," *IEEE Transactions on Biomedical Engineering*, vol. 64, no. 1, pp. 78–86, 2017.

[11] C. Ye, B. V. Kumar, and M. T. Coimbra, "Heartbeat classification using morphological and dynamic features of ECG signals," *IEEE Transactions on Biomedical Engineering*, vol. 59, no. 10, pp. 2930–2941, 2012.

[12] A. S. Alvarado, C. Lakshminarayan, and J. C. Principe, "Time-based compression and classification of heartbeats," *IEEE Transactions on Biomedical Engineering*, vol. 59, no. 6, p. 1641, 2012.

[13] T. Ince, S. Kiranyaz, and M. Gabbouj, "A generic and robust system for automated patient-specific classification of ECG signals," *IEEE Transactions on Biomedical Engineering*, vol. 56, no. 5, pp. 1415–1426, 2009.

[14] S. S. Xu, M.-W. Mak, and C.-C. Cheung, "Towards End-to-End ECG Classification with Raw Signal Extraction and Deep Neural Networks," *IEEE journal of biomedical and health informatics*, 2018.

[15] A. Gogna, A. Majumdar, and R. Ward, "Semi-supervised stacked label consistent autoencoder for reconstruction and analysis of biomedical signals," *IEEE Transactions on Biomedical Engineering*, vol. 64, no. 9, pp. 2196–2205, 2017.

[16] J. Yoo, L. Yan, D. El-Damak, M. A. B. Altaf, A. H. Shoeb, and A. P. Chandrakasan, "An 8-Channel Scalable EEG Acquisition SoC With Patient-Specific Seizure Classification and Recording Processor," *IEEE Journal of Solid-State Circuits*, vol. 48, no. 1, pp. 214–228, Jan 2013.

[17] V. Misra, A. Bozkurt, B. Calhoun, T. Jackson, J. S. Jur, J. Lach, B. Lee, J. Muth, Ö. Oralkan, M. Öztürk *et al.*, "Flexible technologies for self-powered wearable health and environmental sensing," *Proceedings of the IEEE*, vol. 103, no. 4, pp. 665–681, 2015.

[18] W. Tang, A. Osman, D. Kim, B. Goldstein, C. Huang, B. Martini, V. A. Pieribone, and E. Culurciello, "Continuous time level crossing sampling adc for bio-potential recording systems," *IEEE Transactions on Circuits and Systems I: Regular Papers*, vol. 60, no. 6, pp. 1407–1418, 2013.

[19] Association for the Advancement of Medical Instrumentation and others, "Testing and reporting performance results of cardiac rhythm and ST segment measurement algorithms," *ANSI/AAMI EC38*, vol. 1998, 1998.

[20] X. Tang, Q. Hu, and W. Tang, "A Real-Time QRS Detection System With PR/RT Interval and ST Segment Measurements for Wearable ECG Sensors Using Parallel Delta Modulators," *IEEE Transactions on Biomedical Circuits and Systems*, no. 99, pp. 1–11, 2018.

[21] Q. Hu, X. Tang, and W. Tang, "Delta–sigma encoder for low-power wireless bio-sensors using ultrawideband impulse radio," *IEEE Transactions on Circuits and Systems II: Express Briefs*, vol. 64, no. 7, pp. 747–751, 2016.

[22] Q. Hu, X. Tang, and W. Tang, "Integrated asynchronous ultrawideband impulse radio with intrinsic clock and data recovery," *IEEE Microwave and Wireless Components Letters*, vol. 27, no. 4, pp. 416–418, 2017.

[23] W. Tang and E. Culurciello, "A low-power high-speed ultra-wideband pulse radio transmission system," *IEEE Transactions on Biomedical Circuits and Systems*, vol. 3, no. 5, pp. 286–292, 2009.

[24] Y. H. Hu, S. Palreddy, and W. J. Tompkins, "A patient-adaptable ECG beat classifier using a mixture of experts approach," *IEEE transactions on biomedical engineering*, vol. 44, no. 9, pp. 891–900, 1997.

[25] P. de Chazal and R. B. Reilly, "A patient-adapting heartbeat classifier using ECG morphology and heartbeat interval features," *IEEE transactions on biomedical engineering*, vol. 53, no. 12, pp. 2535–2543, 2006.

[26] S. Kiranyaz, T. Ince, and M. Gabbouj, "Real-time patient-specific ECG classification by 1-D convolutional neural networks," *IEEE Transactions on Biomedical Engineering*, vol. 63, no. 3, pp. 664–675, 2016.

[27] A. L. Goldberger, L. A. Amaral, L. Glass, J. M. Hausdorff, P. C. Ivanov, R. G. Mark, J. E. Mietus, G. B. Moody, C.-K. Peng, and H. E. Stanley, "PhysioBank, PhysioToolkit, and PhysioNet: components of a new research resource for complex physiologic signals," *Circulation*, vol. 101, no. 23, pp. e215–e220, 2000.

[28] G. B. Moody and R. G. Mark, "The impact of the MIT-BIH arrhythmia database," *IEEE Engineering in Medicine and Biology Magazine*, vol. 20, no. 3, pp. 45–50, 2001.

[29] S. Kadambe, R. Murray, and G. F. Boudreaux-Bartels, "Wavelet transform-based QRS complex detector," *IEEE Transactions on biomedical Engineering*, vol. 46, no. 7, pp. 838–848, 1999.

[30] S. Barro, M. Fernandez-Delgado, J. Vila-Sobrino, C. Regueiro, and E. Sanchez, "Classifying multichannel ECG patterns with an adaptive neural network," *IEEE Engineering in Medicine and Biology Magazine*, vol. 17, no. 1, pp. 45–55, 1998.

[31] O. E. Liseth, D. Mo, H. A. Hjortland, T. Sverre, D. T. Wisland *et al.*, "Power-efficient cross-correlation beat detection in electrocardiogram analysis using bitstreams," *IEEE transactions on biomedical circuits and systems*, vol. 4, no. 6, pp. 419–425, 2010.

[32] X. Zhang and Y. Lian, "A 300-mV 220-nW event-driven ADC with real-time QRS detection for wearable ECG sensors," *IEEE Transactions on Biomedical Circuits and Systems*, vol. 8, no. 6, pp. 834–843, 2014.

[33] G. Nallathambi and J. C. Principe, "Integrate and fire pulse train automaton for qrs detection," *IEEE Transactions on Biomedical Engineering*, vol. 61, no. 2, pp. 317–326, 2014.

[34] R. Agarwal and S. Sonkusale, "Input-feature correlated asynchronous analog to information converter for ECG monitoring," *IEEE transactions on biomedical circuits and systems*, vol. 5, no. 5, pp. 459–467, 2011.

[35] P. De Chazal, M. O'Dwyer, and R. B. Reilly, "Automatic classification of heartbeats using ECG morphology and heartbeat interval features," *IEEE transactions on biomedical engineering*, vol. 51, no. 7, pp. 1196–1206, 2004.

[36] W. Jiang and S. G. Kong, "Block-based neural networks for personalized ECG signal classification," *IEEE Trans. Neural Networks*, vol. 18, no. 6, pp. 1750–1761, 2007.

[37] M. Llamedo and J. P. Martínez, "Heartbeat classification using feature selection driven by database generalization criteria," *IEEE Transactions on Biomedical Engineering*, vol. 58, no. 3, pp. 616–625, 2011.

[38] F. Alonso-Atienza, E. Morgado, L. Fernandez-Martinez, A. García-Alberola, and J. L. Rojo-Alvarez, "Detection of life-threatening arrhythmias using feature selection and support vector machines," *IEEE Trans. Biomed. Eng*, vol. 61, no. 3, pp. 832–840, 2014.

[39] Q. Li, C. Rajagopalan, and G. D. Clifford, "Ventricular fibrillation and tachycardia classification using a machine learning approach," *IEEE Transactions on Biomedical Engineering*, vol. 61, no. 6, pp. 1607–1613, 2014.

[40] S. Osowski, L. T. Hoai, and T. Markiewicz, "Support vector machine-based expert system for reliable heartbeat recognition," *IEEE transactions on biomedical engineering*, vol. 51, no. 4, pp. 582–589, 2004.

[41] K. H. Lee and N. Verma, "A low-power processor with configurable embedded machine-learning accelerators for high-order and adaptive analysis of medical-sensor signals," *IEEE Journal of Solid-State Circuits*, vol. 48, no. 7, pp. 1625–1637, 2013.

[42] C.-C. Chang and C.-J. Lin, "LIBSVM: a library for support vector machines," *ACM transactions on intelligent systems and technology (TIST)*, vol. 2, no. 3, p. 27, 2011.

[43] G. Moody, B. Moody, and I. Silva, "Robust detection of heart beats in multimodal data: the physionet/computing in cardiology challenge 2014," in *Computing in Cardiology 2014*. IEEE, 2014, pp. 549–552.

[44] Q. Qin, J. Li, L. Zhang, Y. Yue, and C. Liu, "Combining low-dimensional wavelet features and support vector machine for arrhythmia beat classification," *Scientific reports*, vol. 7, no. 1, p. 6067, 2017.

[45] W. Tang, P. M. Furth, V. H. Nammi, G. Panwar, V. Ibarra, X. Tang, G. A. Unguez, and S. Misra, "An aquatic wireless biosensor for electric organ discharge with an integrated analog front end," *IEEE Sensors Journal*, vol. 19, no. 15, pp. 6260–6269, 2019.